Lawrence Berkeley National Laboratory

Lawrence Berkeley National Laboratory

Title

Analysis of the vaporization barrier above waste emplacement drifts

Permalink

https://escholarship.org/uc/item/7162f84t

Authors

Birkholzer, Jens
Mukhopadhyay, Sumitra
Tsang, Yvonne

Publication Date

2003-02-03

Analysis of the Vaporization Barrier above Waste Emplacement Drifts

Jens Birkholzer, Sumit Mukhophadhyay, Yvonne Tsang

Ernest Orlando Lawrence Berkeley National Laboratory,
1 Cyclotron Road, MS 90-1116, Berkeley CA 94720
(510) 486-7134; jtbirkholzer@lbl.gov

Abstract

Prediction of the amount of water that may seep into the waste emplacement drifts is an important aspect of assessing the performance of the proposed geologic nuclear waste repository at Yucca Mountain, Nevada. The repository is to be located in thick, partially saturated fractured tuff that will be heated to above-boiling temperatures as a result of heat generation from the decay of nuclear waste. Since water percolating down towards the repository will be subject to vigorous boiling for a significant time period, the superheated rock zone (i.e., rock temperature above the boiling point of water) can form an effective vaporization barrier that reduces the possibility of water arrival at emplacement drifts. In this paper, we analyze the behavior of episodic preferential flow events that penetrate the hot fractured rock, and we evaluate the impact of such flow behavior on the effectiveness of the vaporization barrier.

1.   Introduction

The performance assessment of underground nuclear waste repositories, such as the proposed repository at Yucca Mountain, Nevada, is supported by prediction of water flow behavior in the unsaturated fractured rock that may be heated to above-boiling temperature from high-level radioactive waste. During the first several hundred years after emplacement, the superheated rock zone above the repository can significantly reduce the possibility of water seepage, forming an effective vaporization barrier. The predicted effectiveness of this barrier depends on the nature of unsaturated flow that is assumed in the simulation models used to analyze thermal-hydrological processes. While process models using continuum assumptions typically predict strongly elevated downward flux towards the superheated rock region as a result of water condensation, this elevated flux does not result in water arrival at the drift during the above-boiling period. However, that the vaporization barrier is predicted to be fully effective in these process models may be in part attributed to the spatial and temporal averaging employed, since the possibility of small-scale flow processes— such as formation of episodic preferential pathways (finger flow)—is underestimated. Different results may be obtained from model concepts that explicitly consider small-scale episodic preferential flow events carrying water at flow rates much larger than average percolation. Such flow events may penetrate far into the superheated rock to eventually reach the waste emplacement drifts.

In this paper, the potential impact of episodic preferential flow events on thermal seepage is studied in a systematic manner. It is assumed that such flow events originate somewhere in the rock region of elevated saturation above the drifts (condensation zone) and percolate downward towards the emplacement drifts. Figure 1a shows an illustration of episodic fingers flowing through fractures and penetrating into the superheated rock above waste emplacement drifts. As flow arrives at the superheated rock region around drifts, water begins to boil off. Depending on the magnitude and duration of each flow event, and the temperature and pressure conditions in the superheated rock, water may completely vaporize above the drift crown, or it may penetrate far into the superheated region and eventually reach the drift. In our study, a semi-analytical solution (Birkholzer, 2002) is used to simulate the complex flow processes of episodic finger flow under thermal conditions. With this solution, the maximum penetration distance into the superheated rock is determined for specific episodic flow events and thermal conditions, and the amount of water arriving at the drift crown is calculated.
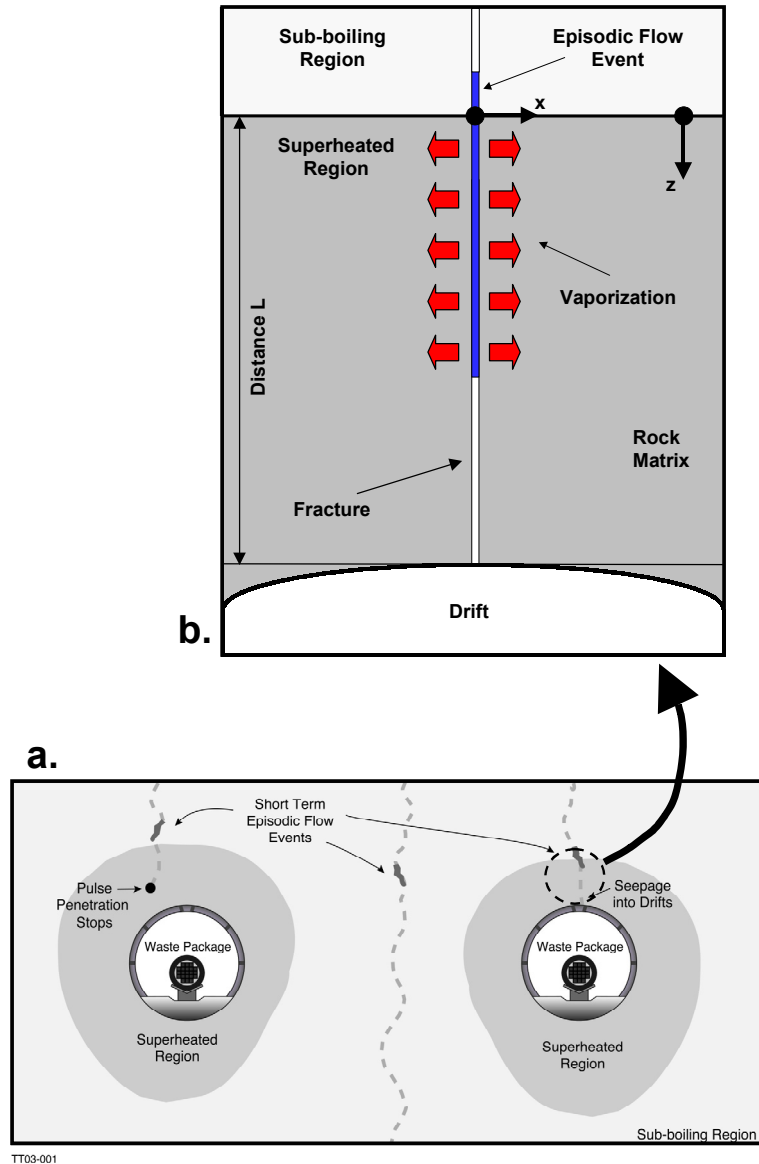
Figure 1. a. Schematic illustration of episodic finger flow in the unsaturated fractured rock surrounding heat-generating nuclear waste packages in emplacement drifts.
b. Conceptual model for finger flow in a vertical fracture above a drift with heat conduction from the adjacent rock.

2.   Conceptual Model

The first step in our analysis is to derive estimates of the potential characteristics of episodic finger flow at Yucca Mountain. Experimental data from a comprehensive laboratory study of Su et al. (1999) are used for this purpose, and a simplified finger-flow model for downward drainage is developed (Section 2.1). The second step is to simulate the fate of such episodic finger-flow events when the flow penetrates into the superheated rock region above waste emplacement drifts, using the semi-analytical solution of Birkholzer (2002). This solution is briefly described in Section 2.2. The solution is implemented at several discrete times after waste emplacement to cover the expected range of rock temperature conditions and the extent of the superheated zone around drifts. These selected times and the respective rock temperature conditions are described in Section 2.3. The third step is to evaluate the results, namely potential for water arrival at the drift at different times after emplacement. The amount of water arriving at the drift crown is evaluated in relation to the perturbed flow situation above the drifts, i.e., in relation to the elevated

downward flux from the condensation zone towards the drift, as simulated from process models using continuum assumptions. Note that water arrival at the drift does not necessarily mean that this water will actually seep into the drift, since the open cavity acts as a capillary barrier, diverting downward flow around the tunnel. This additional barrier caused by capillarity is not considered in the episodic finger-flow model.

2.1   Characteristics of Episodic Preferential Flow

Episodic preferential flow in unsaturated fractures has been experimentally observed in flow visualization experiments using fracture replicas (e.g., Nicholl et al. 1994; Persoff and Pruess 1995; Su et al. 1999). Although constant inlet flow conditions were applied in these experiments, intermittent flow behavior was caused by small-scale capillary barriers within the fracture plane, forming in areas of smaller apertures located above regions of larger apertures. As a result, water accumulated in the small-aperture regions until the water potential exceeded the capillary-force difference. Once this occurred, a large portion of the accumulated water moved rapidly downward in a thin finger. When the capillary pool emptied, the finger snapped and reformed at some later time. Typically, the observed water volumes per event were small, of the order of milliliters.

In our study, we assume that such intermittent flow behavior can also occur in the unsaturated fractures at Yucca Mountain, particularly during the thermal period when condensate above the superheated zone is expected to provide a significant source of water above waste emplacement drifts. Since there are neither experimental studies with fracture test samples from Yucca Mountain nor replicas mimicking Yucca Mountain fractures, we use the flow characteristics observed in the above experiments as estimates for potential episodic preferential flow in unsaturated fractures at Yucca Mountain. Of the experimental studies cited above, the fracture replica analysis of Su et al. (1999) is probably the best suited for this purpose, because the realistic geometry of natural fractures is accounted for, and detailed quantitative measurements are provided in their analysis. The fracture replica in this experimental work was taken from the granitic rock of the Stripa Mine in Sweden. Differences between fractures from the Yucca Mountain tuff and the Stripa Mine granite—with respect to aperture distributions, surface roughness, and contact angle—will bring out differences in flow behavior and distribution. This approach is valid for a qualitative analysis intended to demonstrate the impact of an alternative flow concept on water arrival at the drift during the thermal period at Yucca Mountain.

Su et al. (1999) report a small range of water volumes accumulating in and draining from capillary pools for the entire suite of experiments, fairly unaffected by the order-of-magnitude variation in flow rate imposed at the inlet boundary. Also the width of the rivulets was observed to be independent of the applied flow rate, while the temporal frequency of flow events correlated well with the flow rate at the inlet boundary condition. These observations are consistent with the concept of geometry-induced episodic flow patterns, in which the accumulation and flow distribution of water depends on local aperture variation, while the time between subsequent flow events—required for water accumulation—depends on the rate of overall downward percolation in the fractured rock. Adopting this concept for the thermal conditions at Yucca Mountain, the characteristics of individual fingers draining down from the condensation zone (i.e., finger geometry, water volume per flow event and flow rate) are assumed to be independent of the average downward flux. Their frequency, however, is directly correlated to the average downward flux; i.e., strongly elevated downward fluxes at early stages of heating result in finger flow that occurs more often in time and space.

Basic characteristics defining episodic finger flow, namely water volume of individual flow events V, fracture aperture b, and finger width w, are directly extracted from the experimental results described in Su et al. (1999). Using representative values for these parameters, additional parameters are derived from a simplified conceptual flow model, assuming gravity-driven, laminar, and fully developed flow in vertical one-dimensional channels of uniform width, in fractures of uniform aperture and infinite extent. These derived parameters—flow velocity v_P, mass flow rate m_P, and duration of flow t_P—are input required for the semi-analytical solution described in Section 2.2. (The flow duration denotes the time period needed for the finger to flow past a given location.) Table 1 lists the values extracted from Su et al. (1999) and the calculated flow characteristics of all simulation cases. The so-called Base Case uses the geometric mean values of fracture aperture and water volume given in Su et al. (1999). For finger geometry, Su et al. (1999) report a fairly consistent finger width of about 1 mm, often forming behind advancing water drops that are slightly larger, on the order of 4.5 mm. Since these two values are not sufficient to derive statistical properties, we use the more conservative case with $w = 1$ mm. (Assumptions that potentially lead to higher estimates of water arrival at the drift are considered "conservative" in this paper.) The other cases are

sensitivity cases, adjusting the Base Case value of either fracture aperture or water volume by adding/subtracting the respective standard deviation values (in log space), also extracted from Su et al. (1999). With the water volume and the finger width kept constant, changes in fracture aperture invoke changes in flow velocity, mass flow rate, and flow duration (Cases A and B). A large aperture is associated to a fast, intense, and short flow event. Changes in water volume, while keeping aperture and width constant, only affect the flow duration (Cases C and D). A large volume is related to a long flow duration.

Table 1 Suite of episodic flow events flowing towards the superheated rock region

Simulation Cases	Fracture Aperture b (mm)	Water Volume V (mL)	Finger Width w (mm)	Flow Velocity v_P (m/s)	Mass Flow Rate m_P (kg/s)	Flow Duration t_P (s)
Base Case	0.141	0.161	1.0	0.054	7.3×10^{-6}	21.2
Case A (large aperture)	0.247	0.155	1.0	0.164	3.9×10^{-5}	4.0
Case B (small aperture)	0.081	0.155	1.0	0.018	1.4×10^{-6}	113.4
Case C (large volume)	0.141	0.249	1.0	0.054	7.3×10^{-6}	32.9
Case D (small volume)	0.141	0.104	1.0	0.054	7.3×10^{-6}	13.7
	Extracted from Su et al. (1999)			*Derived using b, V, and w as input*		

2.2 Water Penetration into Superheated Rock

The semi-analytical solution of Birkholzer (2002) is used to determine the maximum penetration distance of episodic fingers subject to vaporization from the hot rock. In case the finger penetrates through the entire superheated zone above the drift, the solution also gives the total amount of water arriving at the drift crown. A brief review of the mathematical formulation and solution procedure is given below. Note that the solution of Birkholzer (2002) is an extension of the analytical solution presented by Phillips (1996). However, Phillips (1996) derived an approximate asymptotic solution for long-term behavior of continuous finger flow, while the semi-analytical solution of Birkholzer (2002) provides an exact simulation method for early and late time periods of flow events that can be episodic or continuous.

The basic conceptual model for the semi-analytical solution of finger penetration into superheated rock is schematically depicted in Figure 1b, showing a superheated region of length L above the crown of a waste emplacement drift. Here, the ambient rock water has been boiled off, and fractures and rock matrix are essentially dry. The rock temperature in the superheated zone is above the boiling temperature at prevailing pressure. Initially, before finger flow occurs, the temperature field is uniform in the lateral x-direction and a function of location in the vertical z-direction. Episodic flow events of given mass flow rate m_P, duration t_P, and finger width w enter the superheated region at $z = 0$ and $t = 0$. The percolating water is already heated to almost boiling temperature T_P upon arrival at the superheated region and begins boiling as it passes the boiling-point isotherm. As presented in the previous section, the downward flow of the finger is gravity-driven and strictly one-dimensional. Upon contact with the water, the rock surface cools to boiling temperature, and a steep temperature gradient is established in the surrounding matrix when the liquid front in the fractures reaches the considered position. With time, the thermal perturbation penetrates further into the rock, the thermal gradient decreases, and heat flow from the matrix to the fracture is reduced. As conduction in the matrix is slow compared to the vertical movement of the liquid pulse, the conductive heat flow within the matrix and from the matrix to the fracture is considered as strictly lateral, perpendicular to the fracture plane.

The downward flow rate at a location z in the superheated region can be derived from a mass balance between the energy required for vaporization of water and the energy supplied by heat conduction from the rock. This mass balance is given in Birkholzer (2002) as follows

$$\frac{\partial m(z,t)}{\partial z} = -\frac{2wk_m}{h} \frac{T_{RI} - T_P}{\sqrt{\pi\kappa(t - t_0(z))}}$$ (Eq. 1)

using an analytical solution of Carslaw and Jaeger (1959) for the lateral temperature distribution in the rock matrix. Here, m(z,t) is mass flow rate at location z and time t, k_m is rock thermal conductivity, h is specific enthalpy of vaporization, T_{RI} is the initial rock temperature, and κ is rock thermal diffusivity. The period $t_0(z)$ denotes the time interval after initial entry of the water finger into the superheated zone until the arrival of the tip of the liquid finger at location z. Equation (1) is valid as long as the thermal perturbation in the rock is nearly uniform across the width of the liquid finger. Since thermal perturbation grows with $(\kappa t)^{1/2}$, the maximum time period t_m associated with uniform thermal perturbation is of order

$$t_m = \frac{w^2}{\kappa} \qquad\qquad (Eq.\ 2)$$

For $t > t_m$, the nearly one-dimensional heat flow perpendicular to the fracture-rock interface transforms to a more circular spreading of heat.

A simple Lagrangian solution scheme was presented in Birkholzer (2002) that solves Equation (1) for episodic flow events of given flow rate and duration. A time-marching procedure tracks the movement of finite water masses traveling downwards while part of the water boils off. The semi-analytical solution scheme was shown to be accurate, robust, and extremely fast. For details on the numerical methods, we refer the reader to Birkholzer (2002).

2.3   Predicted Thermal Conditions at Yucca Mountain

The long-term evolution of thermal-hydrological conditions in the rock is accounted for by applying the semi-analytical solution at 11 selected times after waste emplacement, covering the time period that repository temperatures remain above boiling (about 1,000 years). The thermal parameters required as input for the semi-analytical solution, namely vertical temperature profile and extent of the superheated region, are obtained from drift-scale thermal-hydrological numerical simulations using a multiphase process model, based on a continuum assumption simulating average flow behavior (BSC, 2003). Figure 2 shows results from this model for a drift located in the Topopah Spring middle non-lithophysal unit (Tptpmn), assuming an initial heat load of 1.45 kW/m (average line load measured along drift length) at the time of emplacement. The peak temperature of the rock close to the drift is about 128°C at 75 years after emplacement. The superheated zone is largest between 100 and 450 years of heating, with a maximum extent of 4.19 m above the drift crown. The model simulations indicate that the temperature profile in the superheated region can be approximated by a linear distribution between the maximum temperature at the drift wall and the boiling temperature (i.e., 96 °C) at the top of the superheated rock region. Using this approximation, the rock temperature at each vertical location z in the superheated zone is defined. Note that we apply the same multiphase process model described in BSC (2003) to derive estimates for the thermally induced flow perturbation in the condensation zone above the repository (see Figures 6, 7, and 8).
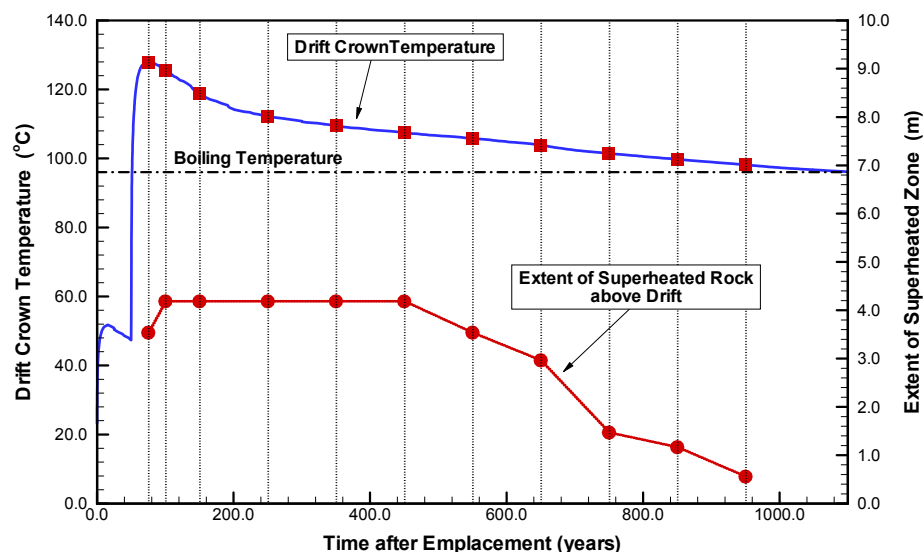

Figure 2.   Predicted wall temperature history in and extent of superheated rock above drifts

3.   Results

3.1   Base Case

To gain a basic understanding of the flow mechanisms of episodic preferential flow events in hot fractures around drifts, we first focus on the Base Case flow event. The semi-analytical solution of Birkholzer (2002) is employed to evaluate the effect of vaporization once this flow event has entered the superheated rock zone. The thermal properties of the rock matrix, required as input to the solution, are based on measured values from the Tptpmn unit. For illustration of results, we choose one time snapshot at 550 years after emplacement. According to Figure 2, the vertical extent of the superheated rock at this time is 3.54 m, with a maximum rock temperature at the drift wall of 105.8^{o}C. Thus, the episodic flow event entering this zone encounters a temperature field of 96°C at a location of 3.54 m above the drift crown, which increases linearly to 105.8^{o}C at the drift wall.

Figure 3 shows the penetration of the tip of the draining finger versus time, with $z = 0$ the top of the superheated domain and $t = 0$ the time when the tip of the finger first enters the boiling zone. (The arrow gives the penetration curve for water flowing with undisturbed velocity $v_P = 0.054$ m/s.) Clearly, after about 2 m, the penetration of the finger slows down noticeably compared to v_P. The farther the finger infiltrates, the stronger this effect is, an effect caused by boiling of water. For illustration purposes, we may use the semi-analytical solution to calculate the maximum penetration of the finger in the absence of the drift opening; i.e., we assume that the superheated fractured rock zone extends further down while the thermal gradient remains the same. In this case, the episodic flow event would end after about 4.17 m, when all water has vaporized. (Note that the time period of finger flow in these cases is longer than the time period t_m according to Equation (2) in which uniform thermal perturbation across the width of the finger can be safely assumed. Applying the semi-analytical solution for times larger than t_m does not account for the more circular spreading of heat in the rock, and therefore underestimates the amount of thermal energy available for boiling of water, leading to a conservative result with respect to the amount of water arriving at the drift crown.)
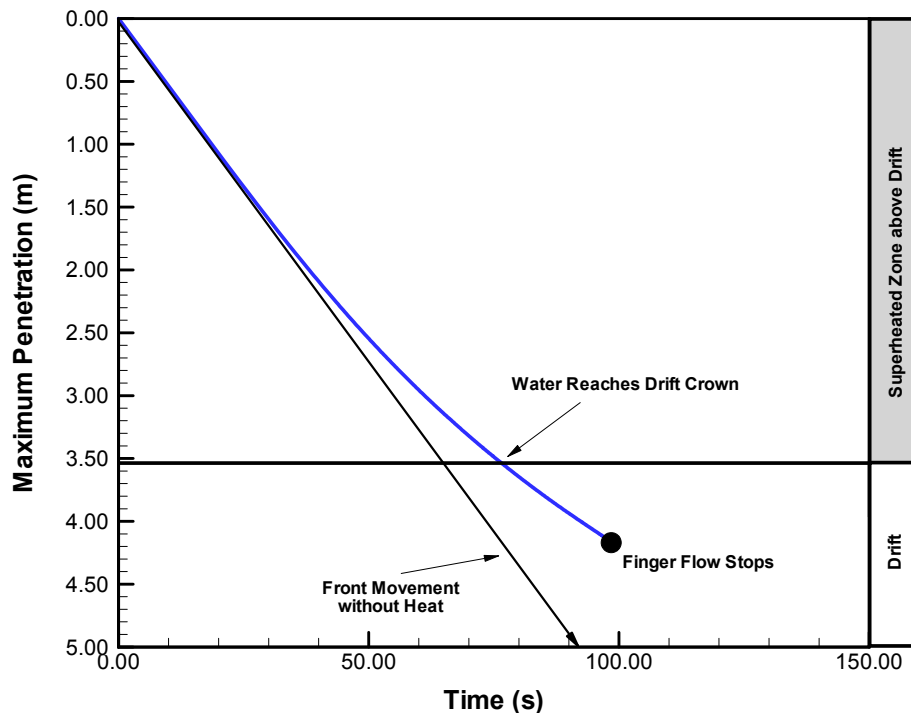

Figure 3.   Maximum penetration of finger tip vs. time at 550 years of heating

After investigating whether episodic preferential flow can overcome the vaporization barrier to arrive at the drift crown, we will now focus our attention on the amount of water reaching the drift. Obviously, the water mass flowing past a given location in the superheated rock decreases with penetration distance, caused by vaporization as

the liquid pulse moves down the fracture. The farther the infiltrating finger penetrates into the superheated region, the less water is available. This is demonstrated in Figure 4, where the total amount of water breakthrough is plotted as a function of vertical penetration distance, given relative to the initial water volume entering the superheated rock. While the major fraction of the initial water volume vaporizes in the superheated rock, about 16.5% of it arrives at the drift crown.

The above results indicate that the relative rate of water arriving at the drift crown is small at 550 years. However, this relative rate needs to be evaluated in conjunction with the flux perturbation in the condensation zone above the repository. Water accumulation in this zone increases the average downward flux towards the superheated zone. Thus, following the conceptual model outlined in Section 2.1, episodic flow events could more frequently—in time and space—originate from the condensation zone, thereby increasing the absolute amount of water arriving at the drift. (It is assumed that the characteristics of individual fingers are not affected by the change in average downward flux). According to results from BSC (2003), the maximum downward flux in the fracture continuum above the drift is about 28 mm/yr at 550 years, which is about 4.6 times higher than the ambient percolation of 6 mm/yr. We may conservatively assume that this elevated flux drains down entirely in an episodic finger-type manner. Then the potential water arrival at the drift crown—including the combined effect of flux elevation and vaporization barrier—can be estimated by multiplying the thermally elevated percolation flux of 28 mm/yr by the relative rate of mass arrival at the drift (from the semi-analytical solution). At 550 years, with 16.5% of the initial water volume arriving at the drift, the resulting flux at the drift crown would be 4.6 mm/yr. Thus, the thermally enhanced downward flux in the condensation zone is effectively reduced by vaporization to a flux rate that is smaller than ambient percolation. While exclusion of water from penetrating down to the drifts may not be absolute at the considered time, the vigorous boiling in the superheated rock still acts as a valuable barrier.
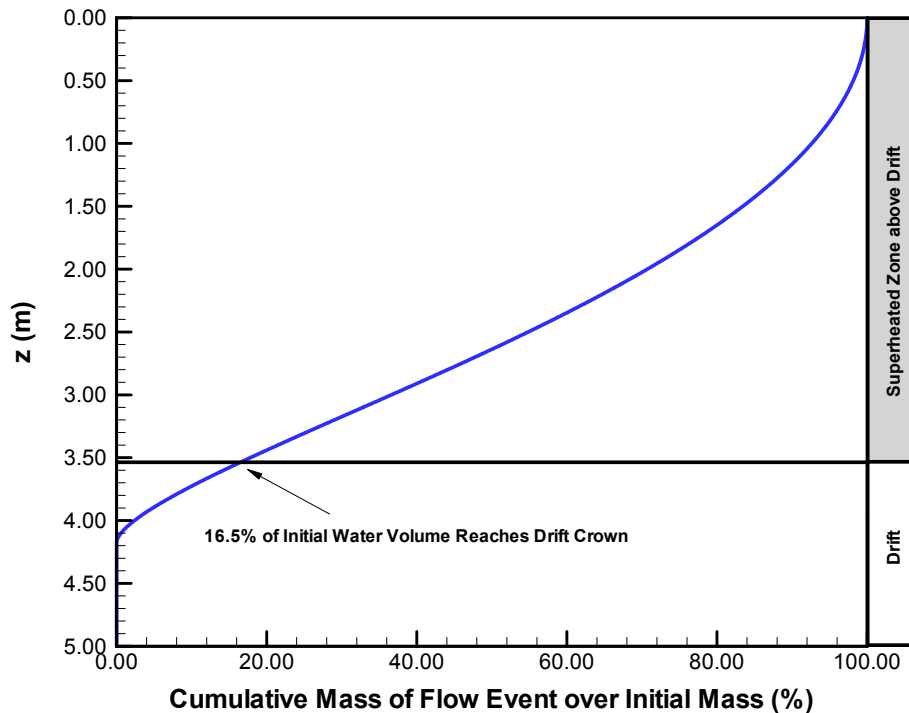

Figure 4.   Total water mass breakthrough at location z at 550 years of heating

The above analysis, conducted for the conditions at 550 years, can be performed for the selected 11 time steps that cover the time period during which rock temperature is above boiling (see Section 2.3). Figure 5 provides results of the semi-analytical solution considering these 11 discrete time steps. The diamond symbols give the maximum penetration distance into the superheated rock, while the circular symbols show the relative amount of water arriving at the drift. The maximum penetration distance should be compared to the dotted curve showing the extent of the superheated region above the drift crown. According to this figure, no water would reach the drift for the first 450

years after emplacement, caused by intense heat and a sufficiently large superheated region. At later times, the possible maximum penetration (in the absence of the drift opening) becomes larger than the boiling zone extent; i.e., water would arrive at the drift crown. The relative amount of water reaching the drift increases significantly between 450 years and 750 years after emplacement, as a result of the decreasing rock temperature and the shrinking superheated rock zone. Eventually, after 950 years, the effect of vaporization becomes marginal, so that the water mass arriving at the drift is almost equal to the initial mass.
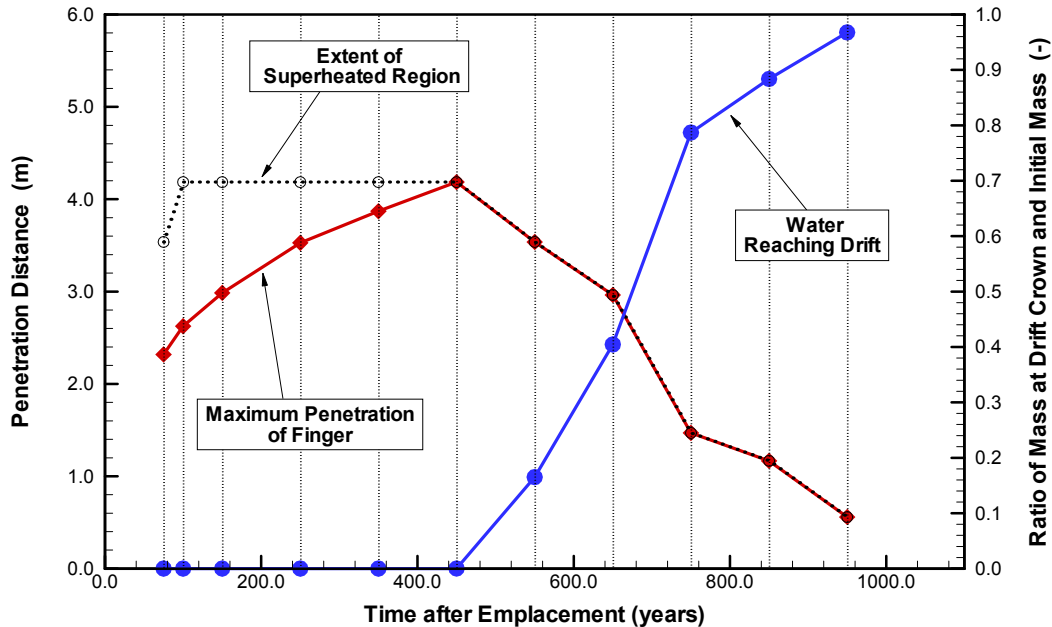
Figure 5.   Maximum penetration and percentage of water mass arriving at drift crown, at 11 different time steps after waste emplacement

In Figure 6, the calculated relative rates of water arriving at the drift crown at the given times are related to the average flux perturbation in the condensation zone at those times. The dashed line shows the so-called flux-elevation factor, which is defined as the maximum downward flux in the condensation zone, divided by the undisturbed ambient percolation. As the circular symbols indicate, the most significant flux elevation occurs at 75 years of heating, where the maximum downward flux is 73.2 mm/yr, more than 12 times that of the ambient flux of 6 mm/yr. Over time, this effect declines rapidly and is essentially negligible at 1,500 years after waste emplacement. (The spike at 650 years is caused by an assumed change in climate at 600 years, leading to an increase in undisturbed ambient percolation at Yucca Mountain.) The solid line gives the water flux arriving at the drift crown when the combined effect of flux perturbation and vaporization barrier is considered. Note that this flux is given relative to the undisturbed ambient percolation at the respective time and is obtained by multiplying the flux-elevation factor with the relative water-arrival rate given in Figure 5. If the displayed values are larger than one, the amount of water potentially arriving at the drift wall exceeds the ambient percolation flux.

It is obvious from Figure 6 that vaporization reduces the impact of flux perturbation in the condensation zone by a large percentage. For the first 450 years of heating, vaporization is so effective that the amount of water potentially arriving at the drift crown is zero. Between 450 and 650 years, vaporization is still strong enough to reduce the elevated fluxes to values smaller than the ambient percolation (i.e., the resulting flux ratio is smaller than one). This clearly demonstrates that the time period of strongly elevated vertical flux in the condensation zone coincides with the time period of very effective vaporization. Thus, even if the downward flux from the condensation zone towards the drift would flow entirely in episodic finger-type patterns—an extreme flow conceptualization that has never been observed at Yucca Mountain—the vaporization barrier would be fully effective for several hundred years. Only at later times, when vaporization effects diminish, is the flux arriving at the drift slightly higher than the natural ambient percolation. However, note that these results are based on many conservative assumptions with respect to

the amount of water reaching drifts, most of them related to the idealized conceptual model of finger flow and heat transport.
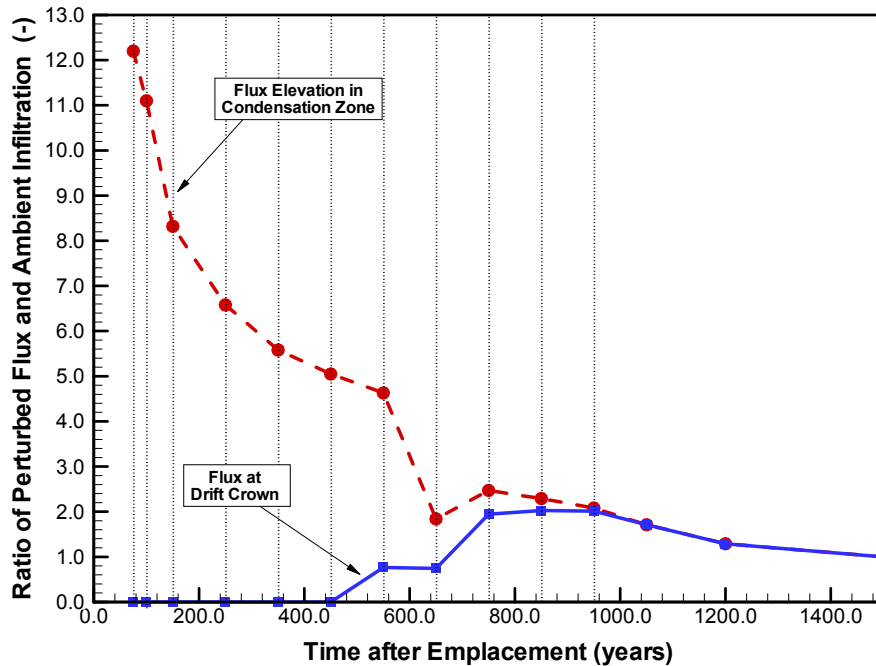

Figure 6.   Ratio of thermally perturbed vertical flux and ambient percolation.

3.2   Sensitivity Cases

Several sensitivity cases are studied to analyze the uncertainty of water arrival at the drift caused by variability in the flow characteristics of episodic finger flow. Of all input parameters required for the semi-analytical solution, those properties related to the small-scale finger-flow characteristics, as extracted from Su et al. (1999), are probably the most uncertain and variable. In contrast, thermal properties of the rock and the future thermal conditions at Yucca Mountain are well constrained by laboratory data, *in situ* measurements, and associated modeling work. Thus in the sensitivity study, we vary fracture aperture and initial water volume per flow event, causing changes in the finger flow properties v_P, m_P, and t_P as given in Table 1. The finger width, the thermal properties of the rock, and the temperature conditions remain unchanged. Results of the sensitivity analysis are given in Figure 7 for Cases A and B (variation of fracture aperture) and Figure 8 for Cases C and D (variation of water volume). The heavy solid and dashed-dotted lines mark the potential water flux at the drift crown—under thermal conditions considering flux elevation and vaporization effects—relative to the undisturbed ambient percolation for cases of large and small aperture (water volume), respectively. For comparison, the thin dotted line shows the respective Base Case results already given in Figure 6.

Fracture aperture is clearly the more sensitive parameter compared to water volume. For both parameters, a change to larger values gives rise to an increased potential for water arrival at the drift. Of all sensitivity cases, Case A is the most critical (large fracture aperture). In this case, the episodic flow event is comparably fast and intense (large velocity and mass flow rate), and the boiling rate of water is limited by the reduced contact time between water and hot rock (small flow duration). However, even then, vaporization in the superheated zone is strong enough to significantly reduce the effect of elevated vertical fluxes draining down from the condensation zone, particularly at early times when the thermal perturbation is largest. The maximum flux elevation ratio at the drift crown is about three at 550 years after emplacement; i.e., the amount of water potentially arriving at the drift would be 18 mm/yr, compared to 6 mm/yr at ambient. This is a relatively small increase that is not expected to result in seepage with the capillary barrier capability at the drift wall accounted for.
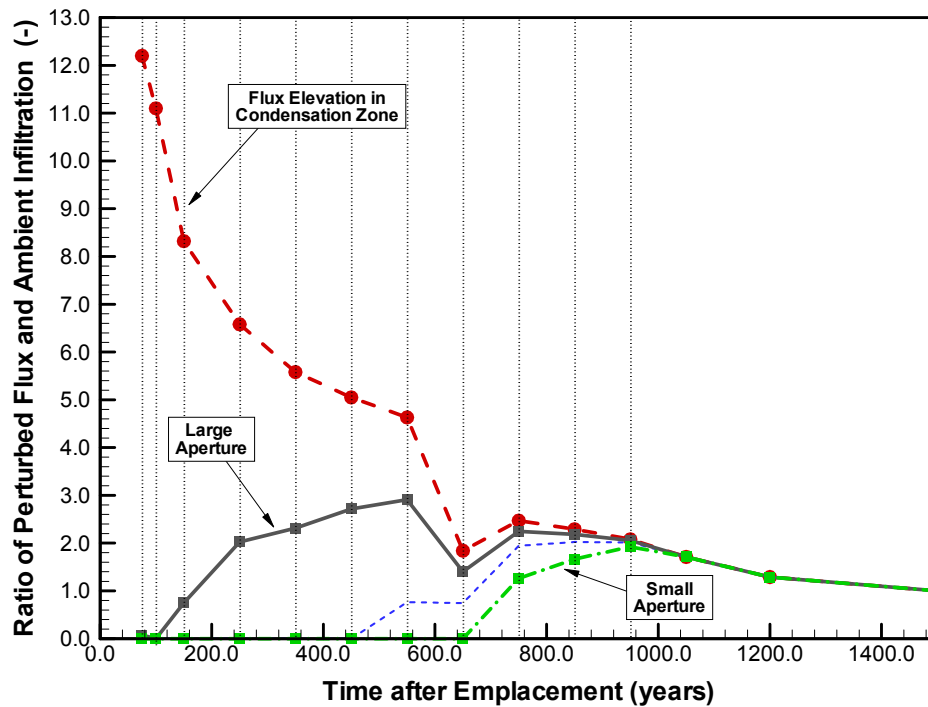
Figure 7. Ratio of thermally perturbed vertical flux and ambient percolation, showing sensitivity of model results to fracture aperture
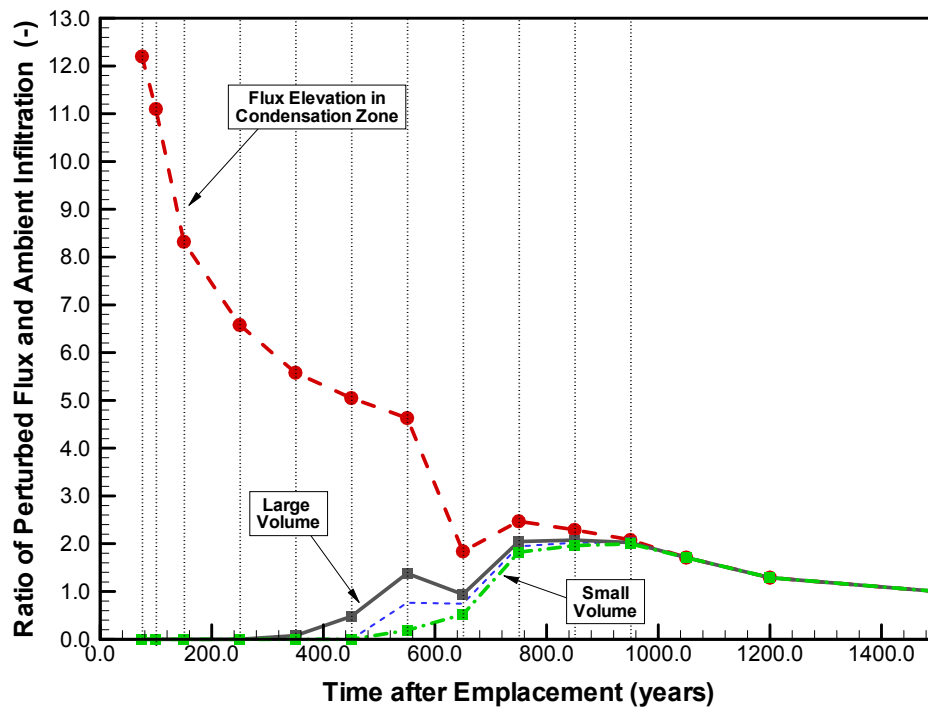

Figure 8. Ratio of thermally perturbed vertical flux and ambient percolation, showing sensitivity of model results to initial water volume

4.   Conclusion and Discussion

Our study analyzes the fate of episodic finger flow penetrating into the superheated rock above emplacement drifts during the time period of strongly elevated temperatures. A semi-analytical solution is utilized to calculate the maximum penetration depth into the superheated rock and, in case the finger flow penetrates down to the drift, to derive the amount of water arriving at the drift wall. The conceptual model is very conservative with respect to the potential for water arrival, since the assumed finger-flow events are fast and intense compared to the average percolation conditions at Yucca Mountain, and since vaporization effects are limited as a result of the small cross-sectional area between the penetrating water and the hot rock. In spite of this conservatism, results of our study demonstrate that finger flow is not able to penetrate through the superheated rock during the first several hundred years of heating, when rock temperature is high and boiling conditions exist in a sufficiently large region above the drifts. These are the conditions in which the largest thermal perturbation occurs, or, in other words, when the potential for episodic finger flow is highest. Only later, when the superheated zone is small and the impact of vaporization is limited, can water arrive at the drift crown. However, the strong thermal perturbation observed at early heating stages has already diminished during this time period, and the net result of water arrival at the drift—considering the combined impact of water buildup in the condensation zone and vaporization in the superheated zone—is similar to ambient percolation rate. Seepage of water into the drift is not expected from this water arrival, because the flow should be effectively diverted around the drift by the the capillary barrier capability of the open cavity.

It is important to realize that the conceptual model in our study includes a number of limiting assumptions that are valid for a qualitative evaluation, but may not be interpreted as a quantitative representation of the system behavior at Yucca Mountain. The most important limitation is that experimental data from a Stripa granite fracture are assumed to represent the characteristics of potential episodic finger flow in fractured tuff at Yucca Mountain. This is a reasonable starting point for demonstration purposes, but will require more experimental work on fractures of Yucca Mountain tuff in the future to confirm the underlying assumptions. Other assumptions, mostly conservative with respect to the simulated penetration distance, are related to the idealized conceptual model of finger flow and heat transport in the superheated rock. In spite of these limitations, our study has elucidated critical parameters and processes that are important in understanding water penetration of finger flow events into superheated fractured rock, and uncertainties inherent in these parameters and processes have been identified.

5.   References

Birkholzer, J.T., TH_PULSE: Program for calculating infiltration of episodic liquid fingers in superheated rock fracture—Theory, user's manual, and sample applications, Rep. LBNL/PUB-3277, Lawrence Berkeley Natl. Lab., Berkeley, CA, 2002.

BSC (Bechtel SAIC Company), Drift-scale Coupled Processes (DST and TH Seepage) Models, MDL-NBS-HS-000015 REV 00, Las Vegas, Nevada, Bechtel SAIC Company, 2003.

Carslaw, H.S., and J.C. Jaeger, Conduction of heat in solids, 2nd ed, Oxford University Press, Oxford, 1959.

Nicholl M. J., R.J. Glass, and S.W. Wheatcraft, Gravity-driven infiltration instability in initially dry nonhorizontal fractures, Water Resour. Res., 30(9), 2533-2546, 1994.

Persoff, P., and K. Pruess, Two-phase flow visualization and relative permeability measurement in natural rough-walled rock fractures, Water Resour. Res., 31(5), 1175-1186, 1995.

Phillips, O.M., Infiltration of a liquid finger down a fracture into superheated rock, Water Resour. Res., 32(6), 1665-1670, 1996.

Su, G.W., J.T. Geller, K. Pruess, and F. Wen, Experimental studies of water seepage and intermittent flow in unsaturated, rough-walled fractures, Water Resour. Res., 35(4), 1019-1037, 1999.